



Swansea University
Prifysgol Abertawe



Cronfa - Swansea University Open Access Repository

This is an author produced version of a paper published in :
Minerals Engineering

Cronfa URL for this paper:

<http://cronfa.swan.ac.uk/Record/cronfa25030>

Paper:

McBride, D., Gebhardt, J., Croft, T. & Cross, M. (2015). Modeling the hydrodynamics of heap leaching in sub-zero temperatures. *Minerals Engineering*

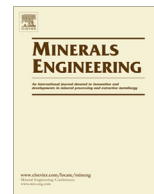
<http://dx.doi.org/10.1016/j.mineng.2015.11.005>

This article is brought to you by Swansea University. Any person downloading material is agreeing to abide by the terms of the repository licence. Authors are personally responsible for adhering to publisher restrictions or conditions. When uploading content they are required to comply with their publisher agreement and the SHERPA RoMEO database to judge whether or not it is copyright safe to add this version of the paper to this repository.

<http://www.swansea.ac.uk/iss/researchsupport/cronfa-support/>

Contents lists available at [ScienceDirect](#)

Minerals Engineering

journal homepage: www.elsevier.com/locate/mineng

Modeling the hydrodynamics of heap leaching in sub-zero temperatures

D. McBride^{a,*}, J.E. Gebhardt^b, T.N. Croft^a, M. Cross^a^a College of Engineering, Swansea University, Singleton Park, Swansea SA2 8PP, Wales UK^b FLSmidth Inc., 7158 S. FLSmidth Drive, Salt Lake City, UT 84047-5559, USA

ARTICLE INFO

Article history:

Received 31 July 2015

Revised 2 November 2015

Accepted 3 November 2015

Available online xxxxx

Keywords:

Heap leaching

Soil hydrodynamics

Freezing and thawing

Modeling

Simulation

ABSTRACT

Heap leaching involves the application of a leach solution onto stacked low grade ores. Solution percolates through the ore, dissolving metals from various minerals, and is recovered at the base. This process is conceptually a simple one, but quickly becomes complex when considering the sub-processes, such as dissolution chemical reactions, oxidation, precipitation, ore with different leaching characteristics, and multi-lift heaps with dynamically changing irrigation schemes.

In addition, changing meteorological conditions, such as heavy rain, evaporation and extreme ambient temperatures have a significant effect on the hydrodynamics. Various factors, such as large variations in ore hydraulic properties, saturated–unsaturated flow, preferential flow pathways, perched water tables, infiltration into dry ore or possible freezing of solution within the heap, can lead to reduced leaching efficiency.

This contribution describes the methods employed within a computational fluid dynamics heap leach model to account for freezing climate conditions. Validation of one-dimensional thermal phase change is performed and a theoretical column of coarse and fine ore is partially frozen to illustrate how the preferred flow path can be counter-intuitive. Finally, a three-dimensional heterogeneous gold oxide ‘test’ heap is simulated assuming non-thermal reactions and sub-zero ambient temperatures. The results demonstrate how recovery can be affected by cold weather changing the hydrodynamics of the heap.

© 2015 Elsevier Ltd. All rights reserved.

1. Introduction

Heap leaching is a process to extract precious metals, such as copper, gold, zinc and uranium, from ore. This is often the preferred method for extracting metal from low grade ore deposits as it provides a low capital cost relative to other methods. Heap leaching typically involves applying a leaching solvent, such as cyanide or acids, over a crushed stockpile of ore; [Bartlett \(1998\)](#) gives an overview of these technologies. A leaching solution containing a reactant is irrigated on to the top exposed surface of the ore. The solution percolates through the heap allowing the reactant to diffuse into the ore particle micro-pores dissolving the metal. The dissolved metal in solution is then transported through the stockpile and drains into collecting ponds at the base of the heap. Solution collected in the ponds is sent for subsequent processing to extract the valuable metals. Heap leaching has been in existence for decades but has evolved over time to a highly controlled process with refined techniques for extracting a range of metals from complex ore deposits in increasingly diverse climates.

[Dhawan et al. \(2012\)](#) provides an overview of heap leaching technology for a range of ore types.

The ideal heap leach location is a temperate semi-arid desert location, such as western U.S. ([Kappes, 2002](#)). However, heap leach operations are frequently located in a range of climates, from tropical to desert climates. Operations located in climates with heavy rains experience tons of water added to the leach system. These heavy rainfalls can change the hydrodynamics of the ore body with systems possibly experiencing strong liquid holdup hysteresis. [Ilankoon and Neethling \(2012\)](#) showed that packed bed experiments suggest that the fluid flow depends not only on the current flow conditions but also on the flow history. Often this additional water is recycled to the heap, for water management purposes, resulting in heaps that act as water storage systems with high phreatic levels. In contrast leach pads can be found in the southern borders of the Sahara desert, where the hot desert climate experiences very little rainfall. High ambient temperatures do not adversely affect leaching kinetics and can lead to increased overall recovery. The use of dripper irrigation requires that only small quantities of water are required, employing good water management practices, water consumption can be less than 0.3 tons of water per ton of ore ([Kappes, 2002](#)). As heap leach technologies have advanced, heap leaching operations have expanded into more

* Corresponding author.

E-mail address: d.mcbride@swansea.ac.uk (D. McBride).

Nomenclature

c	specific heat capacity ($\text{J kg}^{-1} \text{K}^{-1}$)	x	mass fraction (kg kg^{-1})
C	species concentration (mol m^{-3})	z	gravity direction (dimensionless)
B	rate modifier (dimensionless)	<i>Greek symbols</i>	
D	dispersion coefficient ($\text{m}^2 \text{s}^{-1}$)	α	van Guenchten parameter related to the inverse of the air-entry pressure
D_{eff}	effective particle diffusion coefficient ($\text{m}^2 \text{s}^{-1}$)	β	parameter (K)
h	pressure head (m)	γ	surface tension (N m^{-1})
k_{int}	intrinsic permeability (m)	θ	moisture volume fraction ($\text{m}^3 \text{m}^{-3}$)
K	hydraulic conductivity (ms^{-1})	λ	thermal conductivity ($\text{W m}^{-1} \text{K}^{-1}$)
g	gravity (ms^{-1})	μ	liquid viscosity ($\text{kg m}^{-1} \text{s}^{-1}$)
G_{WT}	Gain factor (dimensionless)	ρ	liquid density (kg m^{-3})
L	latent heat of fusion (J kg^{-1})	Ω	impedance factor (dimensionless)
m	mass (kg)	<i>Subscripts</i>	
M	molecular weight of the mineral (kg m^{-3})	a	air
n	van Guenchten parameter related to the pore-size distribution	f	fluid
Q	ratio of ice to liquid ($\text{m}^3 \text{m}^{-3}$)	i	ice
r	radius	j	index
r_m	reacted particle radius	p	matrix
S	sink/source term ($\text{m}^3 \text{s}^{-1}$)	res	residual
t	time (s)	ref	reference value
T	temperature (K)	s	solid
T^*	melting temperature (K)	sat	saturated
u	velocity (ms^{-1})		
VF	volume fraction ($\text{m}^3 \text{m}^{-3}$)		

extreme climates, with leach pads now located in increasingly colder climates. Arctic or near-arctic gold heap leach pads can experience perma-frost with some operations unable to operate during the coldest season. Smith (1997) gives an overview of the problems and operational methods encountered in cold weather. In climates with temperatures falling below zero a significant decrease in recovery can often be seen during these periods. The recovery is normally offset by an increase in recovery during warmer periods and is probably due to solution flowing more slowly as a result of changes to viscosity, surface tension and freezing of solution inside the heap. In addition reaction rates of certain minerals can be thermal dependent thus slowing the recovery.

Adverse flow behavior within the heap is often responsible for low leaching efficiency. Irrigation systems, application rates, migration of fines, heterogeneous materials and compaction can all contribute to complex unsaturated conditions. Seasonal variations, such as rainfall, high and low temperatures, can also have an impact on the flow behavior. Significant rain events can lead to saturated regions within the heap, dilution of the reagent and preferential pathways which wash the leaching solution through, bypassing any reactions with the ore body. Kunkel (2008) states that the recovery of the metal from the ore is influenced more by the solution flow characteristics than the material; in turn, unsaturated flow characteristics in heaps are influenced more by the material than the fluids. Limited and variable solute transport within the heap can significantly affect the leach reaction rates. Unsaturated zone hydrology models and numerical techniques are increasingly being employed to predict and improve the efficiency of the heap by simulating the leaching process to gain an understanding of the flow within the stockpile. A number of authors have employed fluid flow models to investigate the hydrodynamic behavior of the heap, such as Munoz et al. (1997), Bouffard and Dixon (2001), Pantelis et al. (2002), Cariaga et al. (2005), Lima (2006), Peterson and Dixon (2007), Bouffard and West-Sells (2009) and Guzman (2013). Dixon and Petersen (2003) present a method for column heap leaching using a model based on raffinate diffusing out to reaction sites from discrete

channels through the ore and employed comparisons to column test results to generate confidence in the model for predicting behavior in heaps.

Computational Fluid Dynamics (CFD) technologies have enabled more complex multiphase transport in the modeling of the heap leach process (Bennett et al., 2006, 2012; Leahy et al., 2006; Wu et al., 2010; Mostaghimi et al., 2014), but much of this work has been performed employing one-dimensional columns or two dimensional slices. As the hydrodynamics of column tests do not represent the flow behavior on a full scale heap, scale-up of column test recovery to full scale heap recovery is often practiced, but the scale-up factor is dependent upon the hydraulic and physical parameters of the ore so can be very subjective (Scheffel, 2014). A scale up methodology was proposed by Mellado et al. (2011) to predict the effect of heap height and other operation-design variables. Alternatively, full scale simulations can be performed which directly account for ore and hydrodynamic variations within the heap, and McBride et al. (2012a, 2012b) have applied CFD technology to full scale industrial oxide heaps. However, any predictive model requires careful characterization of the ore (McBride et al., 2014a). Advances in material characterization tools and testing techniques allow detailed characterization of ores for simulation based analysis, based on physics, chemistry and material properties. This method directly accounts for material properties changing dynamically within the heap allowing full scale or test heap simulations to be performed to predict the effect of process parameters on recovery (Garcia et al., 2010).

An additional complexity, when modeling large scale heap operations, is capturing the effect of climate and changing meteorological conditions on the heap leach process. Furthermore, the process is never at a steady state, there is usually a combination of ore types with different leaching characteristics, and different irrigation schemes with intermediate solution possibly being recycled to the heap. Climate conditions will have some influence on the hydraulic properties of the ore. At higher temperatures, the surface tension and viscosity of the liquid is reduced. Thus, capillary pressure decreases allowing for the formulation of more

disconnected pathways, higher residual moisture, and the ore becomes more wetttable resulting in an increase in hydraulic conductivity. A number of authors have proposed amendments to the constitutive relationships to account for thermal effects in soils, such as Hopmans and Dane (1986), She and Sleep (1998), Bachmann et al. (2002), Jacinto et al. (2009), and Hanspal and Das (2012). Mathematical models to represent freezing and thawing of solutes in variably saturated soils have emerged from diverse backgrounds resulting in considerable differences in their formulation. Coupled fluid-heat transport in porous media for above freezing and sub-zero temperatures is essential for many agricultural, environmental and soil engineering applications, and indeed in heap leach operations located in cold climates, such as the Arctic regions. However, although the importance of accounting for sub-zero temperatures and the effect of freezing and thawing are widely recognized, there have been limited field studies performed and modeling work has often been confined to one-dimensional analysis. Zhang et al. (2007) employed a one-dimensional frozen soil parameterization study evaluated against observational data from a field study. Gouttevin et al. (2012) presented a one-dimensional soil freezing land-surface flow and energy transport model which is compared against small and large scale field measurements. Three-dimensional models have been developed by a number of authors such as Painter (2011) who developed a three-phase non-isothermal model for water and heat transport in freezing conditions. Dall'Amico et al. (2011) presented a robust model for heat and water flow in freezing variably saturated conditions. Kurylyk and Watanabe (2013) provide a detailed review of the various formulations.

The computational heap leach model employed in this investigation has been developed by coupling variably saturated zone hydrology with CFD technology (McBride et al., 2006) and has been employed to dynamically capture the evolving heap and operational changes (McBride et al., 2012a). The computational procedure for flow is based on the mixed form of the classical Richards' equation, employing an adaptive transformed mixed algorithm (McBride et al., 2006). The model accounts for complex variably saturated flow conditions in porous media, such as infiltration into dry soil, drainage, perched water tables and flow through heterogeneous materials and preferential pathways. Compaction is modeled through permeability functions. The influence of channeling is incorporated into the model by defining regions where a proportion of the solution travels through non-interacting pathways. Precipitation and evaporation are readily modeled by modification of boundary conditions. In this contribution the computational procedure of McBride et al. (2006) is extended to incorporate freezing and thawing. Thermal effects on the ore hydraulic properties have been incorporated into the model (McBride et al., 2014b) by the inclusion of a temperature correction term in the constitutive relationships for pressure-moisture-conductivity (She and Sleep, 1998; Grant, 2003). To account for sub-zero temperatures, where freezing occurs, modifications are made to the mixed form of the Richards equations (Hansson et al., 2004) and for the presence of ice forming in the ore which leads to a blocking effect, an impedance factor is included (Stahli et al., 1996). Amendments to the heap and solute transport equations to account for ice formation are also required and details are given. Functions to relate energy to ice formation are compared and validated against the Stefan analytical solution which is often used to benchmark models that include pore water phase change (Kurylyk et al., 2014). The capture of the evolution of latent heat of phase change is modeled employing the source-based technique commonly used in the melting of metals (Voller et al., 1991). The effect of ice formation on the hydraulic conductivity of the ore and subsequent changes in the preferred flow path is illustrated on a column consisting of coarse and fine material for high and

low application rates. Finally, a 'test' heap comprising a number of materials is leached assuming seasonal temperature variations, including freezing ambient conditions. The heap simulations presented in this paper employ a simple non-thermal gold oxide reaction to investigate the effect of freezing conditions purely on the hydrodynamics of the heap and resulting impact on recovery.

2. Computational model

The computational procedure employed for the solution of unsaturated-saturated flow through porous media is based on the mixed form of the classical Richards equation. The method is numerically robust, employing an adaptive transformed mixed algorithm on a three-dimensional finite volume unstructured mesh framework. A detailed description of the algorithm is given in McBride et al. (2006). A shrinking core concept is employed to model the chemical reactions, consumption of cyanide (CN) from the solution and the extraction of gold (Au), from ore during the leach process. The gold oxide heap leach formulation and numerical solution strategy is given in McBride et al. (2012a). In the following section, details are provided on the adjustments made to the numerical techniques to account for thermal effects, freezing, thawing and blockage due to ice formation.

2.1. Liquid-gas-thermal transport

2.1.1. Variably-saturated flow

The liquid solution for unsaturated-saturated flow through porous media is typically modeled by the mixed form of the Richards' equations (1), which contains terms employing the volumetric moisture content, θ and pressure head, h . In this formulation, the influence of air on the movement of liquid is assumed to be insignificant, thus the gas flow does not influence the liquid flow but the fluid flow can influence the movement of gas. Both the liquid and gas flow can be influenced by temperature gradients where buoyancy forces have a significant influence on the movement of the gas. Oxygen transport between the liquid and gas phase is modeled according to Henry's law, where oxygen liquid-gas transfer is driven by temperature and liquid-gas composition. A detailed description of the interaction between fluid-gas-heat and oxygen transfer is given by Bennett et al. (2012).

$$\frac{\partial \theta}{\partial t} = \nabla[K(h)\nabla h] + \frac{\partial K(h)}{\partial z} + S \quad (1)$$

In Eq. (1), $K(h)$ is the hydraulic conductivity, which is a function of the pressure head (or capillary-suction), z is the direction of gravity, t is time and S is a sink/source term usually representing the boundary conditions or internal preferential flow paths that are represented as sink terms (McBride, 2012a). Modifications are required to the mixed form of the Richards Eq. (1) to account for coupled fluid-heat transport in above freezing and sub-zero temperatures (Hansson et al., 2004), as follows;

$$\frac{\partial \theta_f(h)}{\partial t} + \frac{\rho_i}{\rho_f} \frac{\partial \theta_i(T)}{\partial t} = \nabla[K(h)\nabla h] + \frac{\partial K(h)}{\partial z} + \nabla[K_T(h)\nabla T] + S \quad (2)$$

where the subscripts f and i refer to liquid and ice respectively, ρ is the density and T is the temperature. The density difference between ice and water are often ignored and the total water content is expressed as the sum of the ice and liquid content (Kurylyk et al., 2014). The terms on the right hand side represents fluid flow due to pressure head gradients, gravity and temperature. This formulation assumes that vapor and ice flows are negligible.

2.1.2. Hydraulic properties

Eqs. (1) and (2) are written in terms of two unknown variables, moisture content (θ) and pressure head (h). Hence, to complete the model for variably saturated flow, constitutive relationships for pressure head – liquid moisture content – hydraulic conductivity need to be specified. The unsaturated soil hydraulic properties $\theta(h)$ and $K(h)$ are in general highly nonlinear functions of the pressure head and are often represented by the van Genuchten relationship (van Genuchten, 1980) given in Eqs. (3) and (4);

$$\theta(h) = \begin{cases} \theta_{res} + \frac{\theta_{sat} - \theta_{res}}{[1 + |\alpha h|]^m}, & h < 0 \\ \theta_{sat} & h \geq 0 \end{cases} \quad (3)$$

$$K_{liquid}(h) = K_{sat} \left[\frac{\theta - \theta_{res}}{\theta_{sat} - \theta_{res}} \right]^{0.5} \left[1 - \left(1 - \left[\frac{\theta - \theta_{res}}{\theta_{sat} - \theta_{res}} \right]^{1/m} \right)^m \right]^2 \quad (4)$$

where α and n are material parameters, and $m = 1 - 1/n$. The saturated moisture content is θ_{sat} and residual moisture content after drain down is θ_{res} .

The classical relationships for hydraulic properties are not temperature dependent; however, in reality the temperature of the ore will have some influence on the hydraulic properties. Surface tension and viscosity of the liquid is a function of temperature. Capillary pressure changes can enable higher moisture levels to be retained in open pores. Thus, for lower temperatures there is an increase in surface tension, a decrease in wettability and a reduction in hydraulic conductivity. Conversely, an increase in temperature results in an increase in hydraulic conductivity.

The liquid flow due to a temperature gradient and thermal changes in hydraulic conductivity are given in the third term of the right hand side of the Eq. (2). The hydraulic conductivity K_T is defined as (Hansson et al., 2004);

$$K_T = K_{liquid} \left(h G_{wT} \frac{1}{\gamma_0} \frac{\partial \gamma}{\partial T} \right) \quad (5)$$

where γ is the surface tension of soil water, evaluated as $\gamma = 75.6 - 0.1425T - 2.38 \times 10^{-4} T^2$, γ_0 is the surface tension at 25 °C and G_{wT} is the dimensionless gain factor which depends upon soil properties.

The effect of temperature on the saturated hydraulic conductivity, K_{sat} , mainly depends on the influence of temperature on the liquid viscosity;

$$K_{sat}(T) = \frac{k_{int} \rho_f g}{\mu(T)} \quad (6)$$

where k_{int} is the intrinsic permeability that only relates to pore size distribution and porosity, $\mu(T)$ is the liquid viscosity as a function of temperature and g is gravity. A temperature dependent hydraulic conductivity, $K_{liquid}(h, T)$, is obtained by substituting $K_{sat}(T)$ into Eq. (4).

Grant (2003) reported that capillary pressure is approximately a linear function of temperature. The work reported here employs the temperature correction term proposed by Grant (2003), where Eq. (3) is modified to include a temperature correction term;

$$\theta(h, T) = \begin{cases} \theta_{res} + \frac{\theta_{sat} - \theta_{res}}{[1 + |\alpha h \frac{\beta + T}{\beta - T_{ref}}|]^m}, & h < 0 \\ \theta_{sat} & h \geq 0 \end{cases} \quad (7)$$

where T_{ref} is a base reference temperature and β is an adjustable parameter.

The above formation assumes that as the ice forms in the mushy zone it is uniformly distributed reducing the hydraulic conductivity but not completely blocking the flow path. However, the presence of ice may block pores resulting in a significant increase in the

resistance of the porous media to fluid flow and lead to an apparent blocking effect (Hansson et al., 2004). To account for ice blocking pores, the hydraulic conductivity of the frozen pores is reduced by an impedance factor, Ω , (Stahli et al., 1996). In this formulation the impedance factor is multiplied by the ratio of ice content to total liquid content (Hansson et al., 2004);

$$K(h) = 10^{-\Omega Q} K_{liquid}(h) \quad (8)$$

The parameter Q is the ratio of ice content to the total (minus the residual) liquid content which accounts for the fact that the blocking becomes more significant as the proportion of fluid freezing in the local porous media increases.

2.1.3. Heat transport

Employing the assumption of local thermal equilibrium, a single heat balance equation can be solved for fluid-ice-solid-air matrix, with phase change due to freezing, described as:

$$\frac{\partial}{\partial t} (\rho_p c_p T) + \nabla \cdot (\rho_p c_p \underline{u} T) = \nabla \cdot (\lambda_p \nabla T) + S_T \quad (9)$$

where c_p is the specific heat capacity, λ_p is the thermal conductivity and ρ_p which are defined as in Eqs. (10)–(12), where the fluid, ice, solid and air are represented by the subscript f, i, s, a respectively. A number of authors have employed different methods to estimate the thermal conductivity of variably saturated soils; Hansson et al. (2004) employed a fitted function using six parameters, Leahy et al. (2005) supplemented the thermal conductivity with a thermal dispersivity tensor to give an effective conductivity, Gouttevin et al. (2012) employed an interpolation based on soil saturation. The volumetrically averaged thermal conductivity employed here is based on the inverse of the conductivities of the phases.

$$c_p = \sum_{j=f,i,s,a} \frac{m_j}{m_p} c_j \quad (10)$$

where m_j is the mass of phase j , m_p is the total mass and c_j is the specific heat of phase j .

$$\lambda_p = \frac{m_p}{\sum_{j=f,i,s,a} \frac{m_j}{\lambda_j}} \quad (11)$$

where λ_j is the thermal conductivity of phase j .

$$\rho_p = \sum_{j=f,i,s,a} V F_j \rho_j \quad (12)$$

where $V F_j$ is the volume fraction of phase j .

The source term S_T represents the fluid bulk motion, boundary heat conditions and latent heat of fusion. If only change of phase is considered, the source into the heat equation due to freezing and thawing is;

$$S_T = - \frac{\partial(\rho_i \theta_i L)}{\partial t} - \nabla \cdot (\rho_i \underline{u} \theta_i L) \quad (13)$$

where L is the latent heat of fusion and θ_i is the ice fraction which is a function of temperature.

In soil freezing models Eq. (13) is usually incorporated into the apparent heat capacity term, c_p in Eq. (9). However this method requires very small time step with steep soil freezing curves, as a large time step can produce a temperature change that misses the latent heat evolution. The model reported in this paper employs source based techniques taken from the metals solidification community (Voller et al., 1991) where the phase change energy is captured in a source term allowing larger time step sizes to be employed. For numerical stability, the ice is often assumed not to form instantaneously but is typically represented by a function that depends on the liquidus temperature, T_f , which is the temperature at which the liquid contains no ice and the solidus

temperature, T_s , which is the temperature at which the liquid is totally frozen. The simplest form of this function assumes a piecewise linear relationship between temperature and ice fraction such as;

$$\theta_i = \begin{cases} 0 & T > T_f; \text{ the liquidus temperature} \\ \theta & T < T_s; \text{ the solidus temperature} \\ \frac{T-T_s}{T_f-T_s}\theta & T_s \leq T \leq T_f; \text{ in the mushy zone} \end{cases} \quad (14)$$

The phase change is typically linearly represented over a temperature interval of 2 °C (Gouttevin et al., 2012). When employing the piecewise linear freezing curve the total freezable liquid can be considered as $\theta - \theta_{res}$ (Kurylyk et al., 2014). An alternative method for evaluating the phase change is to assume thermodynamic equilibrium conditions and employ a form of the Clapeyron equation (Kurylyk et al., 2013). Employing the commonly accepted assumption that soil freezing behaves as soil drying then the ice pressure can be set to zero and a generalized Clapeyron equation can be employed, allowing the variation of liquid pressure head during phase change to only be dependent on water temperature (Dell'Amico et al., 2011). This assumption is reasonable provided that freezing induced mechanical deformation is not considered (Kurylyk et al., 2013). Thus under freezing conditions the liquid pressure head can be written as;

$$h_f(T) = \begin{cases} h + \frac{1}{gT^*}(T - T^*); & \text{if } T < T^* \\ h; & \text{if } T \geq T^* \end{cases} \quad (15)$$

where g is gravity and T^* provides the melting temperature under freezing conditions. The melting temperature can be calculated as:

$$T^* = T_f + \frac{gT_f}{L}h \quad (16)$$

The total liquid content, θ_f , can be obtained by substituting $h = h_f(T)$ into Eq. (7) and the ice fraction, θ_i , is given as;

$$\theta_i = \theta(h, T) - \theta_f(h_f(T), T) \quad (17)$$

2.1.4. Solute transport

The continuity equation for the convective–dispersive transport of multiple solutes in variably saturated flows is given by,

$$\frac{\partial(\theta C_j)}{\partial t} - \nabla \cdot (\theta_f D_f \cdot \nabla C_j) + \nabla \cdot (q C_j) = S_j \quad (18)$$

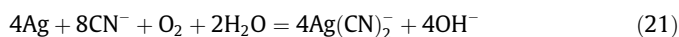
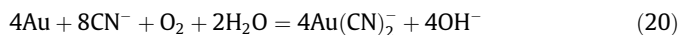
where C_j is the concentration of species j in the solution phase and S_j the production or consumption of species j . D is the dispersion coefficient and q is the modified Darcy flux,

$$q = -K_{liquid}(h, T)\nabla h \quad (19)$$

The hydraulic conductivity, $K_{liquid}(h, T)$, is a property of the porous media porosity and the viscosity of the fluid which is temperature dependent. Thus, the variably saturated hydraulic conductivity is a function of both pressure and temperature.

2.2. Reaction chemistry

In the simulations presented in this paper a simple gold oxide mineral is leached using the following stoichiometry;



The dissolution of species from solid to liquid state is tracked explicitly by a shrinking core algorithm, per particle class. The

ore is characterized by defining a representative particle size distribution, each size class being assigned individual mineral properties. The local chemistry balance per unit volume is determined by summing the reaction products for each particle size fraction and scaling according to availability of reactants. Typically for a gold oxide material, the chemical reactions occur between cyanide in solution and the oxide minerals in the solid phase. The rate of change in reacted particle is modeled assuming instantaneous chemical reaction with diffusion rate limiting, as

$$\frac{dr_m}{dt} = \frac{1}{4\pi r_m^2 B} \frac{M_j}{\rho x_j} R_{diff} \quad (23)$$

where r_m is the characteristic reacted particle radius.

B relates to the chemical leaching reaction.

ρ is the particle density.

M_j is the molecular weight of the mineral.

x_j is the mass fraction of the mineral.

The chemical reaction rate modifier, B , is constant for all particle size classes and needs to be determined, experimentally or by calibration, for each mineral. As reaction rates differ for each ore type, the value of B is best determined for each ore from column test data. The diffusion rate limiting, or resistance term, R_{diff} is given by,

$$R_{diff} = -4\pi D_{eff} r_m^2 \frac{dc}{dr} \quad (24)$$

where D_{eff} is the effective particle diffusion coefficient and dc/dr is the concentration of cyanide over the radius of the particle.

3. Freezing test cases

The thermal-freezing process is validated against the Stefan analytical solution. This allows the model to be validated using idealized boundary conditions, uniform heat conductivity, λ and constant volumetric water content θ . The Stefan solution (25) gives the progression of the freezing front (z) with time (t).

$$z = \sqrt{2 \cdot \lambda \cdot \frac{(T_s - T_f)}{\theta \cdot L \rho_f} \cdot t} \quad (25)$$

where $T_s - T_L$ is the temperature difference from the top surface to the freezing front.

Then a theoretical column containing a coarse and fine material is investigated in order to illustrate how freezing affects the hydraulic conductivity and resulting flow path in heterogeneous material. As the hydraulic conductivity is dependent upon the degree of saturation and the capillary suction increases as the moisture in the ore decreases, the preferred flow path is often counter-intuitive and will switch between coarse and fine material dependent upon application rate (O'Kane, 1999).

3.1. Thermal-freezing validation

The Stephan solution (25) provides validation for one-dimensional unsaturated soil phase change. For this case a column of unsaturated ore containing a uniform volume fraction of 0.19 $\text{m}^3 \text{m}^{-3}$ liquid is initially at just above freezing at 0 °C. At time $t = 0$, the top surface is reduced to -6 °C and all other surfaces are insulated. The thermal conductivity, λ , is set to 1.05 $\text{W m}^{-1} \text{K}^{-1}$.

Several simulations were run employing different liquid–temperature relationships. The first employed a linear relationship between the temperature and fraction of liquid content. Two simulations were performed, firstly with a freezing interval of 1 °C and secondly with a freezing interval of 5 °C. For these initial simulations all the liquid is assumed to freeze at the freezing

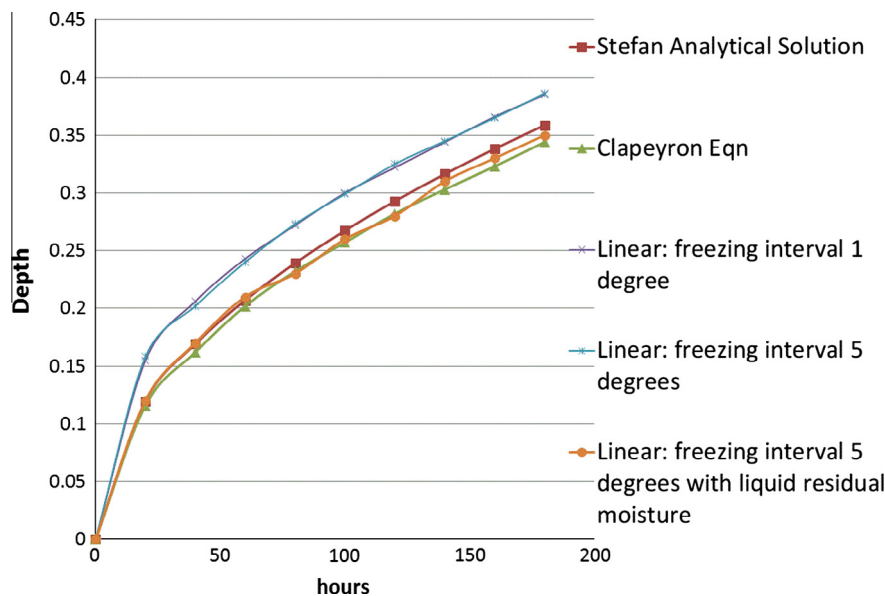


Fig. 1. Freezing front progression.

temperature. For both these simulations the freezing front is slightly overestimated, as can be seen in Fig. 1. A second simulation is run with a freezing interval of 5 °C but with the assumption that the total ice content is the liquid content less the residual moisture. This assumption gives a better match to the analytical results. Lastly, the simulation is run employing the generalized Clapeyron equation and (17) to predict the phase change. Fig. 1 shows the freezing front predicted for all the methods along with the analytical solution. All the methods give a reasonable prediction of the freezing process with the freezing interval of 5 °C with liquid residual moisture giving the best match. For the rest of the simulations reported in this paper this method will be employed.

3.2. Preferential flow path

A theoretical column of ore, segregated down the axis of the column, contains fine material on the left side and coarse material on the right side. There is no barrier to lateral flow across the interface of the fine and coarse material. The materials have a saturated hydraulic conductivity of 1.0×10^{-1} m/s and 5×10^{-5} m/s for the coarse ore and the fine ore respectively. Solution is applied uniformly to the top surface of the column and recovery of solution is measured at the base of the coarse ore and at the base of the fine ore. Evidently, for saturated material the preferred flow path will be the coarse ore. For unsaturated material, as in heap leaching, the preferred flow path will depend upon the flux rate applied at the top of the column and the material properties of the ore. For application rates above the saturated hydraulic conductivity of the fine ore, liquid will preferentially travel through the coarse ore. For application rates below the saturated hydraulic conductivity of the fine ore, the preferred flow path will depend on the capillary suction of the ore. Fig. 2 shows the hydraulic conductivity functions for the fine and coarse material. As can be seen in Fig. 2, at application rates below 4×10^{-6} m/s the fine material has the higher capillary suction and becomes the preferred flow path. Model verification was performed employing two higher application rates, 10^{-4} m/s and 10^{-5} m/s and two lower application rates, 10^{-6} m/s and 10^{-7} m/s. Fig. 3 shows the flow paths and saturation levels after 1 day for the highest and lowest application rate. The simulated results predict the correct flow path and are comparable to the experimental results of O’Kane (1999).

3.2.1. Temperature effects

The simulations were repeated assuming that firstly, the coarse material is partially frozen and secondly the fine material is partially frozen. The partially frozen material was held in a uniform ‘mushy’ state, without total blocking of flow. The new hydraulic conductivity functions for each case is shown in Fig. 4 and the percentage of solution collected at each outlet is shown in Table 1. As can be seen in Table 1, for an application rate of 10^{-5} m/s the solution switches from flowing preferentially in the coarse ore to the fine ore when ice forms in the coarse material. Conversely, when the finer material was partially frozen the solution switched from preferentially flowing through the finer material to the coarse material.

4. Leaching simulations

Finally, simulations are performed on a heterogeneous ‘test heap’ containing a gold oxide ore with the same mineralogy and six-class particle size distribution but with a varying percentage of fines. The reaction parameters are obtained by calibrating the model against 4 m column test data with the assumption of constant saturated hydraulic conductivity of 5.0×10^{-5} m/s. In the ‘test’ heap the hydraulic conductivity is assumed to vary by depth which is typical for large heaps. The ‘test’ heap is leached over a one-year period assuming (1) above zero temperature fluctuations, (2) Seasonal temperature variation with above-, near- and sub-zero temperatures. Solution path and recovery is analyzed at three collection outlets.

4.1. Parameterization

The reaction kinetics for the gold oxide ore employed in the ‘test’ heap simulation were obtained by calibration of the model to column test data. Details of the calibration process can be found in McBride et al. (2014a). The reaction parameters for the shrinking core reaction (23) and a dummy cyanide consumer is calibrated to match the cyanide consumption due to other oxide minerals such as silver and copper that were not explicitly tracked. Fig. 5 shows the calibrated models’ predicted recovery against experimental column test data.

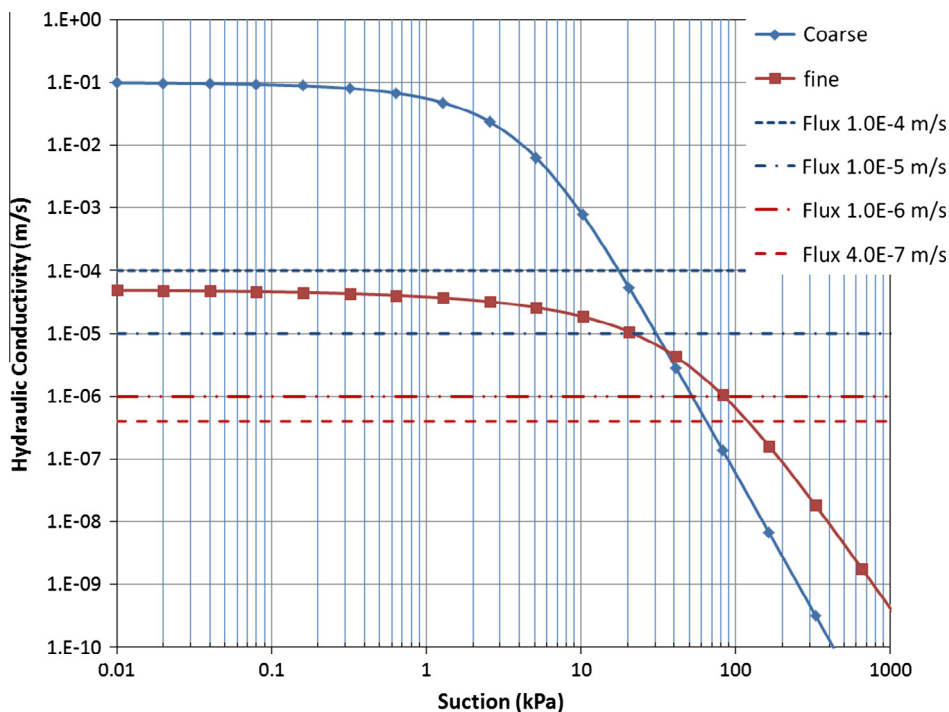


Fig. 2. Hydraulic functions for the fine and coarse ore.

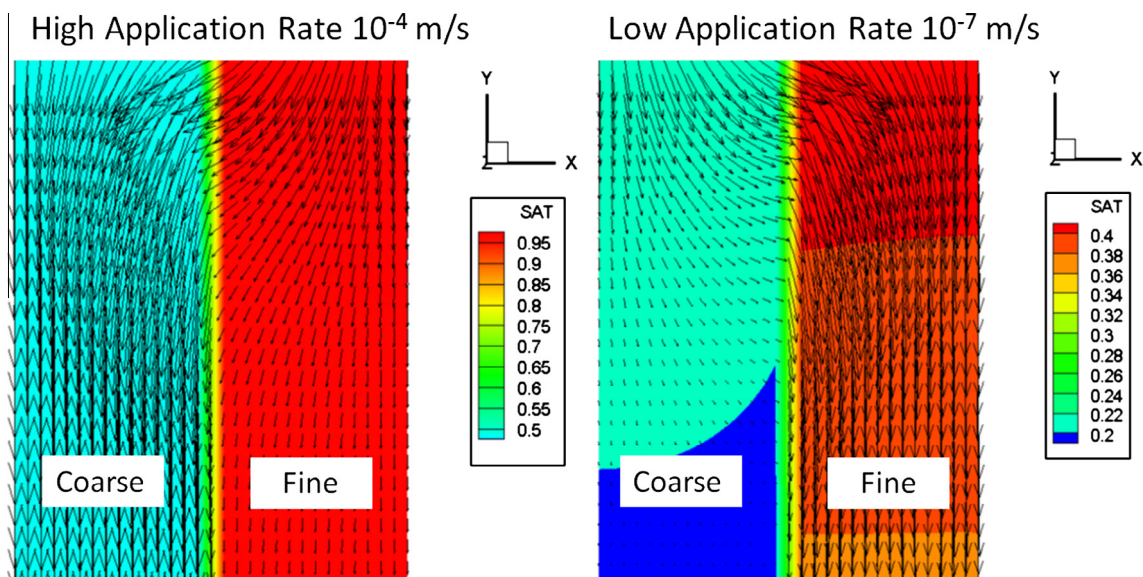


Fig. 3. Flow paths and saturation levels for uniform application rates.

4.2. Test heap simulation

The three-dimensional 'test' heap was analyzed with respect to changing thermal conditions. The heap consisted of the gold oxide ore containing other cyanide consuming minerals, such as silver and copper. The other minerals were not explicitly tracked but accounted for in the simulations as 'Other CN – consumers'. The particle distribution and gold grade is shown in Table 2. The heap has dimensions of 40 m by 60 m and consists of three lifts; each lift contains three materials with 15%, 20%, and 25% fines. The lifts were split into six cells of dimensions 20 m by 20 m by 18 m, with hydraulic properties varying by depth to allow for compaction. Saturated hydraulic conductivity and van Genuchten parameters for

ore at various depths within the heap are shown in Fig. 6 for ore with 15%, 20% and 25% fines. These relationships were obtained from in-situ and laboratory testing.

The heap was irrigated with a leaching solution of 50 ppm cyanide at a constant rate of 5 L/m²/h for the 3 front lifts and 10 L/m²/h for the 3 back lifts. Fig. 7a shows the ore stacking arrangement. The cyanide solution was uniformly applied to Lift 1 for 90 days. Lift 2 was then stacked on top of Lift 1, and leaching solution was uniformly applied to Lift 2 for another 90 days. Finally, Lift 3 was stacked on top of Lift 2, and was leached for a further 180 days. Fig. 7b) shows the base meteorological data that was applied to all external boundaries of the heap. New lifts were assumed to be instantaneously stacked so that the ore was continuously irrigated.

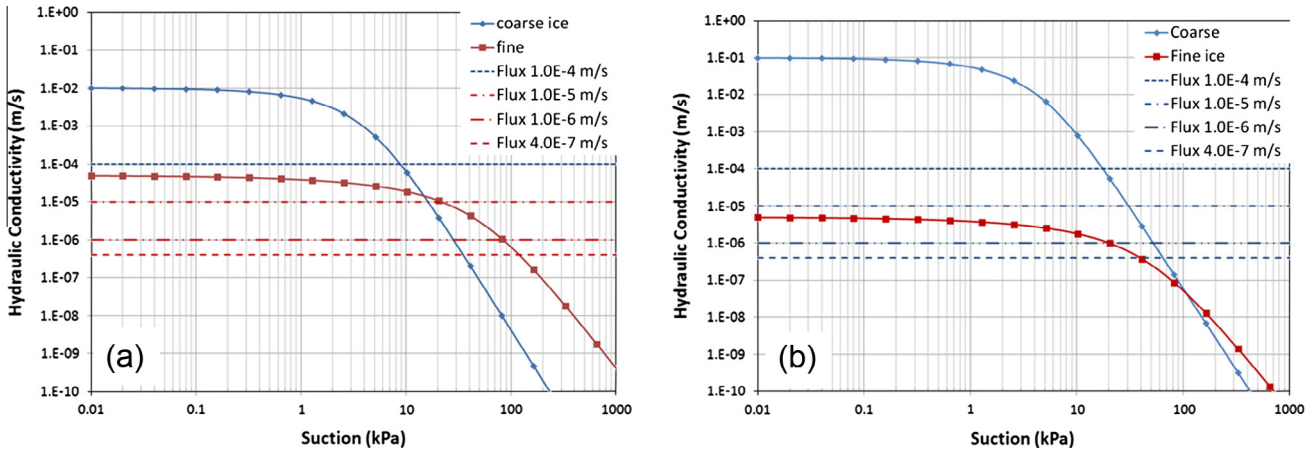


Fig. 4. Hydraulic function comparison with partially frozen material (a) coarse (b) fine.

Table 1
Percentage of solution recovered from coarse or fine material.

Flux (m/s)	No freezing		Freezing coarse		Freezing fine	
	Coarse (%)	Fine (%)	Coarse (%)	Fine (%)	Coarse (%)	Fine (%)
10 ⁻⁴	89	11	86	14	99	1
10 ⁻⁵	59	41	34	66	93	7
10 ⁻⁶	13	87	4	96	71	29
10 ⁻⁷	8	92	1	99	54	46

Preferential flow channels were assumed not significant until placement of the third lift. Any solution traveling through preferential pathways was collected at the nearest outlet. Distinct outlets were located at the base of each ore type; Outlet 1 at the base of the ore containing 15% fines, Outlet 2 associated with the 20% fines material and Outlet 3 for the 25% fines material.

Initially, the simulation was run with the base meteorological data, shown in Fig. 7b. Solution volume and gold concentration were tracked at the outlets. The temperatures in the first six months were reduced by 10 °C, increasing again to the base temperature for the remaining six months to simulate a seasonal climate change. Comparison of the volume of solution recovered is given in Fig. 8a for all outlets, where the dashed line is the recovery for the base temperatures and solid line is the recovery for the sea-

sonal change in temperature. As can be seen in Fig. 8a, in the first six months the volume of solution recovered from Outlet 2, which has fewer exposed surfaces, has increased and the volume of solution recovered from Outlets 1 and 3 has reduced. This was due to increased solution retained within the heap, Fig. 8b, and an increase in solution traveling through non-frozen internal regions. At the end of the first six months the percentage distribution of the total solution collected is 27%, 39% and 34% per Outlet 1, 2 and 3 respectively, compared to the base solution collected distribution of 30%, 35% and 35%. The recoverable solution contained within the heap was similar toward the end of the simulation when temperatures increased and ice had thawed. As can be seen in Fig. 8a, there is a marked increase in solution recovered at all three outlets during the thaw. Fig. 9 shows contour and iso-surface plots of the liquid fraction and ice fraction at the end of the first six months for the seasonal simulation. Fig. 9b also includes three cross-sections through the heap showing liquid fraction contours internal to the heap. As can be seen in Fig. 9a, most of the liquid near the exposed heap surfaces has frozen. Internally, there is no ice but liquid fractions are higher than seen in the base simulation, with moisture levels near saturation compared to a maximum of 80% saturated seen in the base simulation.

The reduced temperatures in the seasonal simulation resulted in a reduction in gold recovered, during the first quarter by 6%, second quarter by 7% and end of year by 4%. The increase in solution

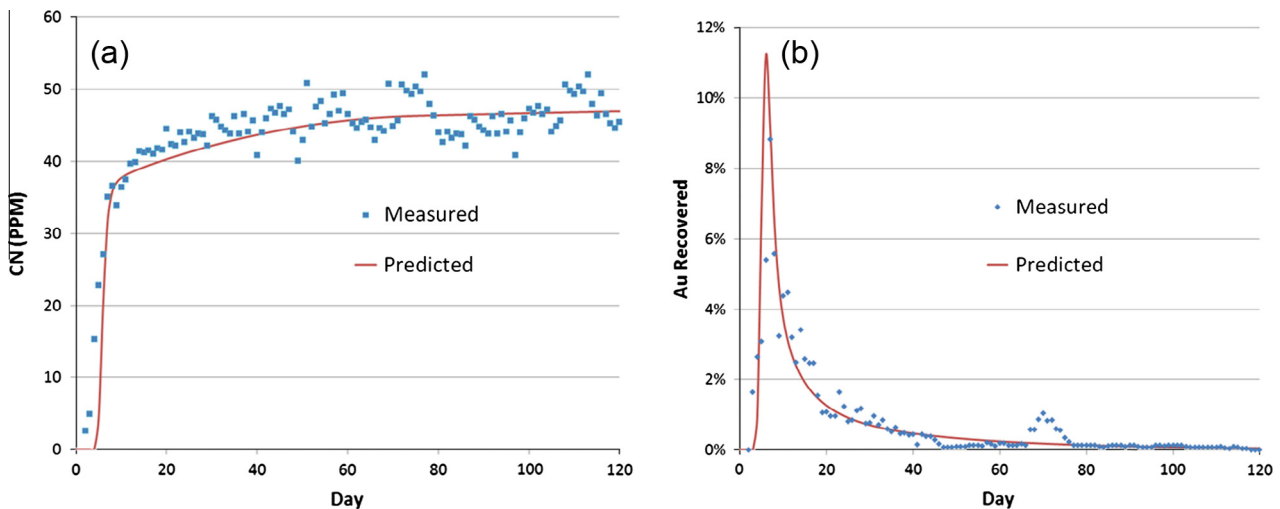


Fig. 5. Predicted recovery against measured recovery (a) cyanide (b) gold.

Table 2
Ore grade and particle size distribution.

Screen	Weight distribution (%)	Au (g/t)	Other CN- consumers (g/t)
-12"	14.3	0.68	100.00
-6"	4.7	0.74	100.00
-4"	6.2	0.70	100.00
-3"	14.7	0.67	100.00
-2"	15.5	0.56	100.00
-1"	44.5	0.54	100.00

inventory in the heap accounts for approximately 4% of the difference, Fig. 10a). As shown in Fig. 10b) the gold concentration in the recovered solution slightly increased at outlets 1 and 2 during the first six months. However, during the second quarter the gold concentration reporting to outlet 3 significantly reduced. This can also be seen in Fig. 11b) where there is an increase in gold inventory in this region. Flow in this region was restricted by low hydraulic conductivity and had the largest percentage of ice. Fig. 11 shows the

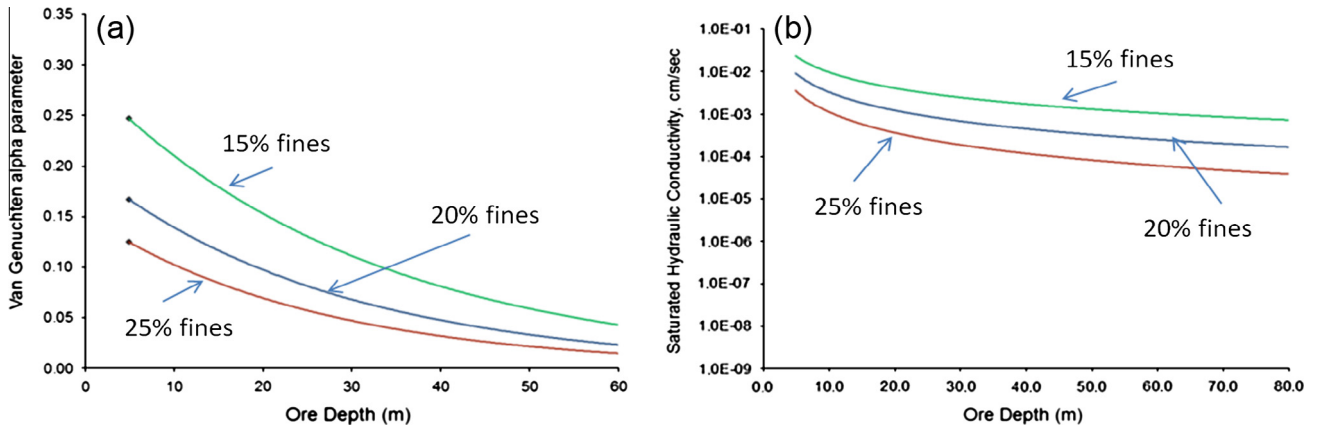


Fig. 6. (a) van Genuchten parameters and (b) saturated hydraulic conductivity.

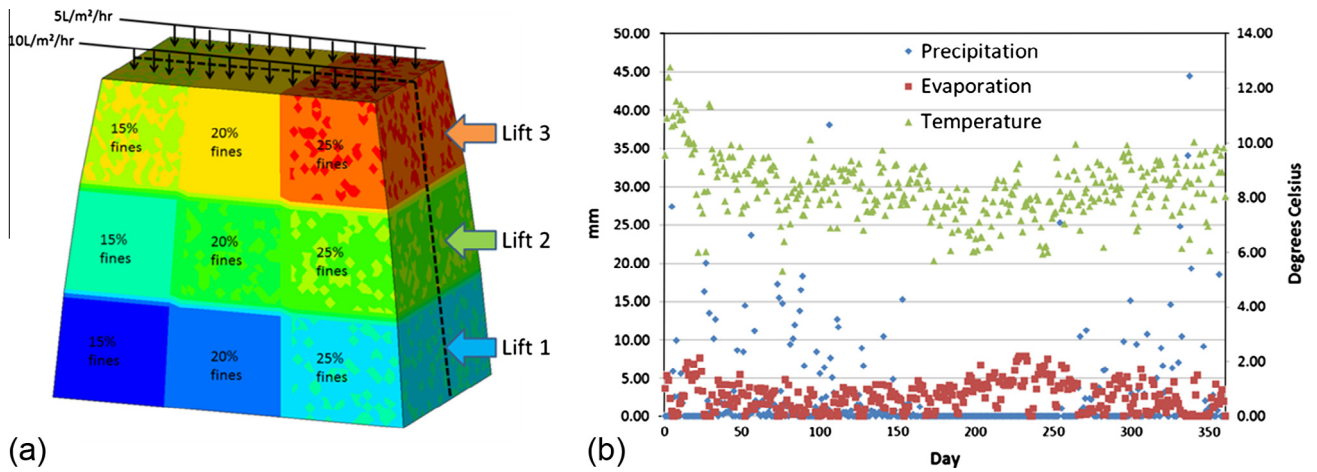


Fig. 7. (a) Stacking of lifts and materials (b) base meteorological data.

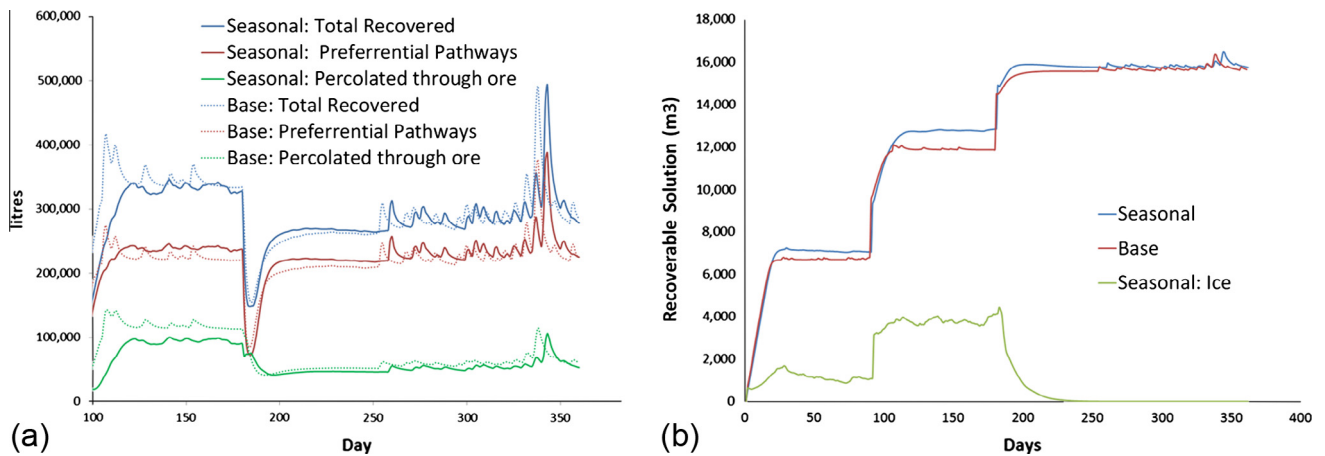


Fig. 8. (a) Solution recovered by outlet (b) recoverable solution inventory in heap.

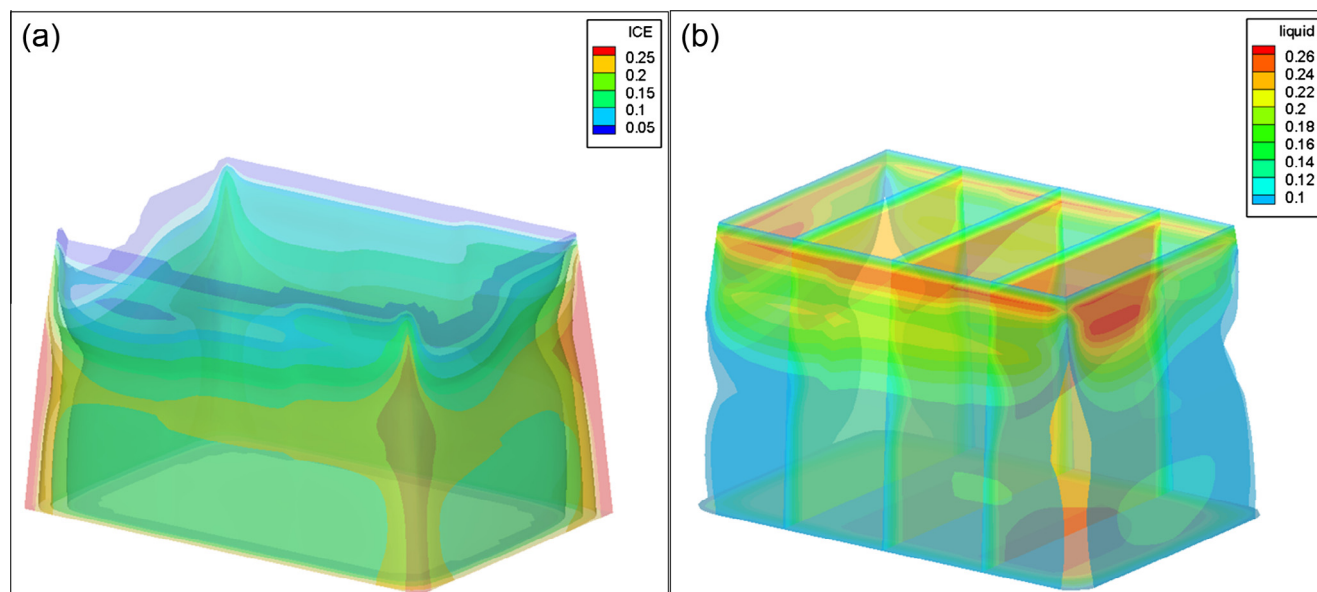


Fig. 9. Seasonal simulation (a) volume fraction of ice (b) volume fraction of liquid.

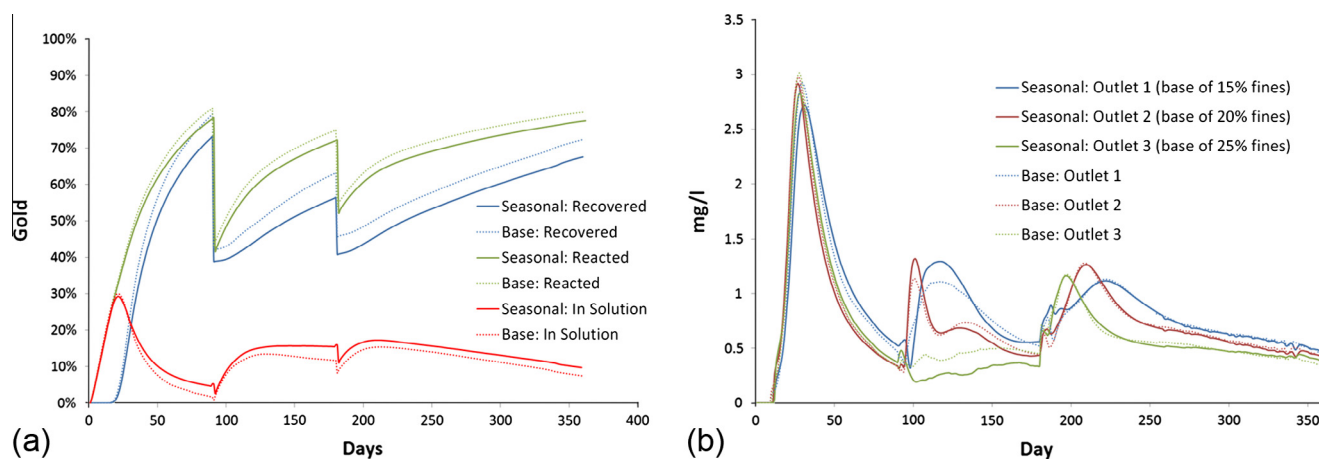


Fig. 10. Gold (a) percent of total available, (b) in solution per outlet.

gold inventory after six and twelve months for both the base simulation and seasonal simulation. Higher residual grades were obtained for the seasonal simulation with an increase in gold inventory of 4% in the first six months. However, some of this was offset by a slightly increased recovery in the second six months with the difference in gold inventory reducing to 2%.

One half of the heap had leaching solution applied at a rate of 10 L/m³/hr and the other half at a rate of 5 L/m³/hr, as shown in Fig. 7a). At the end of six months, under freezing conditions, the gold inventory in the ore receiving the higher application rate was 11.72% lower than the ore receiving the lower application rate, compared to the base simulation where it was 9.52% lower. The 2.2% increase in gold reacting in the ore receiving the higher flow rate was mainly seen in the ore body closest to the boundaries. The 25% fines material inventory reduced the most giving a 1.6% inventory reduction under the higher flow rate in freezing conditions. The gold inventory in the 15% and 20% fines material reduced by 1% and 0.6% respectively. The 20% fines material had fewer exposed boundaries and was therefore less affected by freezing.

5. Conclusions

For real-world leaching predictions, full scale heap simulations must account for changing meteorological conditions and diverse climates. Temperature variations, evaporation, rainfall, freezing and thawing can significantly affect the hydrodynamics of the heap and influence recovery. Changes in the hydraulic properties result in non-uniform and diverse internal flow conditions, even for uniform solution application rates. Freezing conditions can restrict recovery through reduced availability of reactant and an increase in solution inventory followed by an increase in drain down and recovery on thawing. Many of these complex flow conditions are successfully accounted for in the comprehensive model reported here. Amendments to the variably saturated flow, heat and solute transport equations to account for sub-zero temperatures have been implemented. Temperature effects on capillary pressure and the local hydraulic properties of the ore are also incorporated into the model. The periodic behavior of freezing and thawing within the heap can alter the flow paths and distribution of active flow channels in the heap leaching system. To some extent the blocking

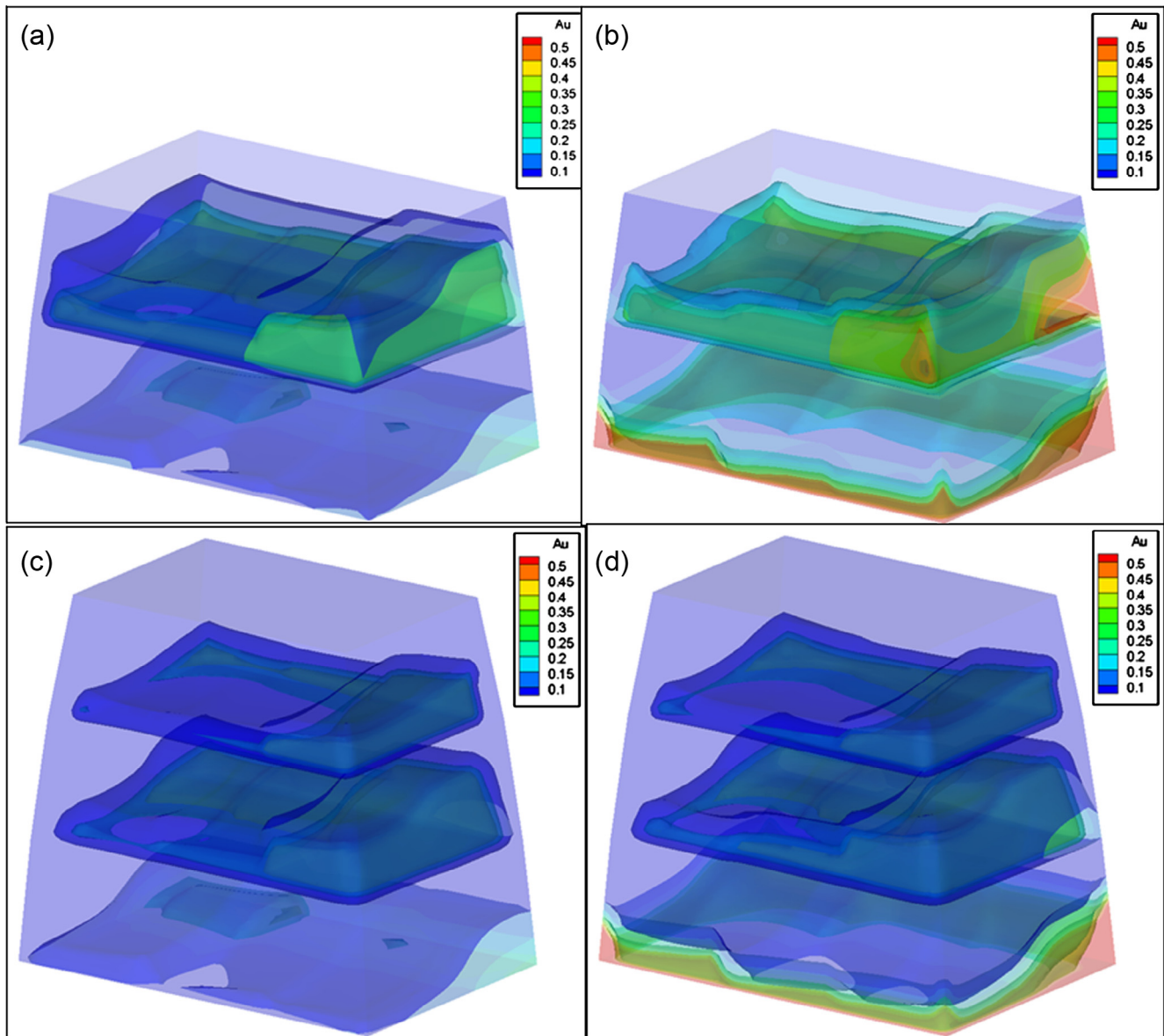


Fig. 11. Gold inventory (Au g/t) (a) base after 6 months, (b) seasonal after 6 months, (c) base after 1 year, (d) seasonal after 1 year.

of existing flow paths is accounted for within the model by employing an ice impedance factor which forces the creation of new flow paths through the ore. This may result in the creation of additional flow channeling and liquid dynamics hysteresis, not presently accounted for in the model, which in turn will influence recovery.

Simulations have been performed to illustrate how different application rates, ore types and thermal conditions affect the movement of solution through the ore. Changing thermal conditions have been shown to alter the preferred flow path. The study reported in this paper illustrates the effect of temperature and percent fines on the hydraulic performance of a hypothetical 'test' heap. The simulations illustrate that cold weather can affect recovery not only by limiting thermal chemical reactions but by altering the flow path and increasing the solution inventory. Freezing weather conditions can reduce recovery and the simulations reported here indicate that the reduction in recovery may be limited by adjusting the irrigation rate. Any optimal changes in operating conditions for extreme weather conditions will very much

depend on the heap system and ore body under investigation. However, for the hypothetical heap reported here, employing a higher irrigation rate during freezing weather may reduce ice formation and increase recovery. Increasing the temperature of the applied solution may also improve leaching efficiency but this has not been investigated in this study.

The model also allows for a wide array of complex thermo-liquid–solid chemical reactions. In the simulations reported here a simple isothermal gold oxide reaction has been employed to focus on the thermal effects of the hydraulic properties. However, the model will be applied to a more complex sulfide leach in a future contribution. These thermo-chemical reactions can create local temperature variations that can impact the local hydrodynamics of the ore. Given the size and highly complex nature of the heap system, many ore properties and dynamically changing network of preferential flow channels, the model predictions should be viewed in qualitative terms rather than hard quantities. However, the model could provide trends in recovery for various operating conditions during diverse weather conditions for different ore

bodies, thus providing a tool to investigate the sensitivity of recovery to changing heap conditions, whether meteorological, structural and/or operational.

References

- Bachmann, J., Horton, R., Grant, S.A., van der Ploeg, R.R., 2002. Temperature dependence of water retention curves for wettable and water-repellent soils. *Soil Sci. Soc. Am. J.* 66, 44–52.
- Bartlett, R.W., 1998. *Solution Mining*, second ed. Gordon and Breach Science Publishers, Amsterdam, Netherlands.
- Bennett, C.R., McBride, D., Cross, M., Gebhardt, J.E., Taylor, D.A., 2006. Simulation technology to support base metal ore heap leaching. *Miner. Process. Extract. Metall.* 115 (1), 41–48.
- Bennett, C.R., McBride, D., Cross, M., Gebhardt, J.E., 2012. A comprehensive model for copper sulphide heap leaching: basic formulation and validation through column test simulation. *Hydrometallurgy* 127–128, 150–161.
- Bouffard, S.C., Dixon, D.G., 2001. Investigative Study into the hydrodynamics of heap leaching processes. *Metall. Mater. Trans. B* 32, 763–776.
- Bouffard, S.C., West-Sells, P.G., 2009. Hydrodynamic behavior of heap leach piles: influence of testing scale and material properties. *Hydrometallurgy* 98, 136–142.
- Cariaga, E., Concha, F., Sepulveda, M., 2005. Flow through porous media with applications to heap leaching of copper ores. *Chem. Eng. J.* 111, 151–165.
- Dall'Amico, M., Endrizzi, S., Gruber, S., Rigon, R., 2011. A robust and energy-conserving model of freezing variably-saturated soil. *The Cryosphere* 5, 469–484.
- Dhawan, N., Safarzadeh, M.S., Miller, J.D., Moats, M.S., Rajamani, R.K., Lin, C., 2012. Recent advances in the application of X-ray computed tomography in the analysis of heap leaching systems. *Miner. Eng.* 35, 75–86.
- Dixon, D.G., Petersen, J., 2003. Comprehensive modelling study of chalcocite column and heap bioleaching. Montreal, Canada. In: Riveros, P.A., (Ed.) et al., *Hydrometallurgy of Copper*, Proceedings of Copper, 6, pp. 493–516.
- Garcia, S., Ramon, C., Espin, A., Gebhardt, J.D., Hernandez, A., McBride, D., Cross, M., 2010. Gold heap leach simulation and optimization using a multiphysics model. *Miner. Metall. Process. J.* 27 (4), 196–204.
- Gouttevin, I., Krinner, G., Ciais, P., Polcher, J., Legout, C., 2012. Multi-scale validation of a new soil freezing scheme for a land-surface model with physically-based hydrology. *The Cryosphere* 6, 407–430.
- Grant, S.A., 2003. Extension of temperature effects model for capillary pressure saturation relations. *Water Resour. Res.* 39 (1), 1003.
- Guzman, A., Robertson, S., Calienes, B., 2013. Constitutive relationships for the representation of a heap leach process. In: van Zyl, D., Caldwell, J. (Eds.), *Proceedings of the Heap Leach Solutions Conference*, Vancouver, B.C., pp. 442–458.
- Kappes, D.W., 2002. Precious metal heap leach design and practice. In: *Proceedings of the Mineral Processing Plant Design, Practice, and Control*, Society for Mining, Metallurgy, and Exploration, Littleton, CO, pp. 1606–1630.
- Hansson, K., Simunek, J., Mizoguchi, M., Lundin, L.-C., van Genuchten, M.T., 2004. Water flow and heat transport in frozen soil: numerical solution and freeze-thaw applications. *Vadose Zone J.* 3, 693–704.
- Hanspal, N.S., Das, D.B., 2012. Dynamic effects on capillary pressure–Saturation relationships for two-phase porous flow: implications of temperature. *AIChE J.* 58 (6), 1951–1965.
- Hopmans, J.W., Dane, J.H., 1986. Temperature dependence of soil hydraulic properties. *Soil Sci. Soc. Am. J.* 50, 4–9.
- Jacinto, A.C., Villar, M.V., Roberto, G.E., Ledesma, A., 2009. Adaptation of the van Genuchten expression to the effects of temperature and density for compacted bentonites. *Appl. Clay Sci.* 42 (3/4), 575–582.
- Kurylyk, B.L., Watanabe, K., 2013. The mathematical representation of freezing and thawing processes in variably-saturated, non-deformable soils. *Adv. Water Resour.* 60, 160–177.
- Kurylyk, B.L., McKenzie, J.M., MacQuarrie, K.T.B., Voss, C.I., 2014. Analytical solutions for benchmarking cold regions subsurface water flow and energy transport models: one-dimensional soil thaw with conduction and advection. *Adv. Water Resour.* 70, 172–184.
- Kunkel, J., 2008. Heap leach lixiviant flow myth versus reality tailings and mine waste. *Design Operation and Disposal*. CRC Press, pp. 63–72.
- Ilankoon, I.M.S.K., Neethling, S.J., 2012. Hysteresis in unsaturated flow in packed beds and heaps. *Miner. Eng.* 35, 1–8.
- Leahy, M.J., Davidson, M.R., Schwarz, M.P., 2005. A model for heap bioleaching of chalcocite with heat balance: bacterial temperature dependence. *Miner. Eng.* 18 (13), 1239–1252.
- Leahy, M.J., Schwarz, M.P., Davidson, M.R., 2006. An air sparging CFD model of heap bioleaching of chalcocite. *Appl. Math. Modell.* 30, 1428–1444.
- Lima, L.R.P.de Andrade, 2006. Liquid axial dispersion and holdup in column leaching. *Miner. Eng.* 19, 37–47.
- McBride, D., Cross, M., Croft, T.N., Bennett, C.R., Gebhardt, J.E., 2006. Computational modelling of variably saturated flow in porous media with complex three-dimensional geometries. *Int. J. Num. Meth. Fluids* 50, 1085–1117.
- McBride, D., Gebhardt, J.E., Cross, M., 2012a. A comprehensive oxide heap-leach model: development and validation. *Hydrometallurgy* 113–114, 98–108.
- McBride, D., Cross, M., Gebhardt, J.E., 2012b. Heap leach modelling employing CFD technology: a 'process' heap model. *Miner. Eng.* 33, 72–79.
- McBride, D., Croft, T.N., Cross, M., Bennett, C., Gebhardt, J.E., 2014a. Optimization of a CFD – heap leach model and sensitivity analysis of process operation. *Miner. Eng.* 63, 57–64.
- McBride, D., Gebhardt, J.E., Cross, M., 2014b. Investigation of hydrodynamic flow in heap leaching using a CFD computational model. In: 7th International Symposium on Hydrometallurgy, Victoria, Canada
- Mellado, M.E., Casanova, M.P., Cisternas, L.A., Galvez, E.D., 2011. On scalable analytical models for heap leaching. *Comput. Chem. Eng.* 35 (2), 220–225.
- Mostaghimi, P., Tollit, B.S., Neethling, S.J., Gorman, G.J., Pain, C.C., 2014. A control volume finite element method for adaptive mesh simulation of flow in heap leaching. *Eng. Math.* 87 (1), 111121.
- Munoz, J., Rengifo, P., Vauclin, M., 1997. Acid leaching of copper in a saturated porous material: parameter identification and experimental validation of a two-dimensional transport model. *J. Contam. Hydrol.* 27, 1–24.
- O'Kane, M., Barbour, S.L., Haug, M.D., 1999. A Framework for Improving the Ability to Understand and Predict the Performance of Heap Leach Piles, Copper99–Cobre99. In: Young et al (Eds.), *The Minerals, Metals and Materials Society*, Vol IV, 409–419.
- Painter, S.L., 2011. Three-phase numerical model of water migration in partially frozen geological media: model formulation, validation, and applications. *Comput. Geosci.* 15, 69–85.
- Pantelis, G., Ritchie, A.I.M., Stepanyants, Y.A., 2002. A conceptual model for the description of oxidation and transport processes in sulphidic waste rock dumps. *Appl. Math. Modell.* 26, 751–770.
- Petersen, J., Dixon, D.G., 2007. Modelling zinc heap bioleaching. *Hydrometallurgy* 85, 127–143.
- Scheffel, R.E., 2014. Heap leach development – Achieving the correct conceptual design – Part 11. In: *Proceedings of Heap Leach Solution*, Lima, Peru.
- She, H.Y., Sleep, B.E., 1998. The effect of temperature on capillary pressure-saturation relationships for air-water and perchloroethylene-water systems. *Water Resour. Res.* 34 (10), 2587–2597.
- Stahli, M., Jansson, P.-E., Lundin, L.-C., 1996. Preferential water flow in a frozen soil – a two-domain model approach. *Hydrol. Process.* 10, 1305–1316.
- Smith, K.E., 1997. Cold-weather gold heap-leaching operational methods. *JOM: J. Min. Metals Mater. Soc.* 49 (4), 20–23.
- Van Genuchten, M.Th., 1980. A closed-form equation for predicting the hydraulic conductivity of unsaturated soils. *Soil Sci. Soc. Am. J.* 44, 892–898.
- Voller, V.R., Swaminathan, C.R., 1991. General source-based method for solidification phase change. *Num. Heat Trans., Part B* 19, 175–189.
- Wu, A., Liu, J., Yin, S., Wang, H., 2010. Analysis of coupled flow-reaction with heat transfer in heap bioleaching processes. *Appl. Math. Mech., Eng. Ed.* 3 (12), 1473–1480.
- Zhang, X., Sun, S., Xue, Y., 2007. Development and testing of a frozen soil parameterization for cold region studies. *J. Hydrometeorol.* 8, 690–701.